HHS Public Access

Author manuscript

J Interv Card Electrophysiol. Author manuscript; available in PMC 2018 January 23.

Published in final edited form as:

J Interv Card Electrophysiol. 2001 December ; 5(4): 391–400.

Comparison of Irrigated Electrode Designs for Radiofrequency Ablation of Myocardium

Deeptankar Demazumder[1], **Mark S. Mirotznik**[2], and **David Schwartzman**[1]

[1] Electrophysiology Research Laboratory, Allegheny University of the Health Sciences, Philadelphia, PA

[2] Department of Electrical Engineering, Catholic University of America, Washington, DC

Abstract

Background—Previous reports have demonstrated that radiofrequency energy delivered to myocardium via an irrigated electrode results in a more voluminous ablation lesion than a non-irrigated electrode. Different irrigated electrode designs have been utilized; no direct comparisons have been reported.

Purpose—To compare different irrigated electrode designs.

Methods—Three irrigation electrode designs were compared to a control (non-irrigated electrode) group: 1. internal; 2. showerhead; 3. sheath. For each electrode, prior to ablation Doppler echocardiographic assessment of the irrigant flow along the electrode outer surface was performed. Ablation was performed *in vitro* utilizing a whole blood-superfused system. Electrode, electrode–endocardial interface, and intra-myocardial temperatures were assessed, as were ablation circuit impedance, total delivered energy, and lesion and electrode morphology. Room temperature normal saline was utilized as the irrigating fluid, delivered at 20 cc/min. Electrode–endocardial interfacial blood flow was assessed at rates of 0 and 0.26 m/s.

Results—Irrigant was contained within the internal electrode design and therefore the electrode outer surface manifested no significant flow during irrigation. Irrigant spread primarily radially away from the showerhead electrode design, yielding relatively high electrode outer surface flow at the irrigation holes, but low elsewhere. Irrigant traveled in parallel to and enveloped the electrode outer surface of the sheath electrode design, yielding relatively moderate but uniform flow.

Ablation via each of the irrigated electrodes yielded greater ablation energy deposition and larger lesion dimensions than the non-irrigated electrode. Irrigation did *not* necessarily prevent interfacial boiling, which could occur during uninterrupted radiofrequency energy deposition and lesion growth. The results for the 3 irrigation designs were incongruent. The duration of radiofrequency energy application via the internal electrode design was significantly shorter than the other designs, curtailed by impedance rise. This yielded the smallest total radiofrequency energy

Address for correspondence: David Schwartzman, MD, Atrial Arrhythmia Center, University of Pittsburgh, Presbyterian Hospital B535, 200 Lothrop Street, Pittsburgh, PA 15213-2582., schwartzmand@msx.upmc.edu.

Data presented in part at the 18th annual scientific sessions of the North American Society of Pacing and Electrophysiology, New Orleans, LA, 1997

deposition and smallest ablation lesion volume. Relative to this, duration using the showerhead design was significantly longer, associated with greater total energy deposition and larger lesion volume. The sheath design permitted the longest duration, associated with the largest total energy deposition and lesion volume.

Conclusions—Although each of the irrigated electrode designs yielded larger lesions than the non-irrigated electrode, they were not comparable. Ablation duration and lesion size were directly correlated with flow along the electrode outer surface.

Keywords

catheter ablation; radiofrequency; ablation; myocardium; irrigation

Previous investigators have documented that radiofrequency energy applied to myocardium via an irrigated electrode yields deeper and more voluminous ablation lesions than with a non-irrigated electrode; this is associated with a higher cumulative applied energy [1–5]. It has been concluded that the irrigation creates a larger lesion in part by cooling the electrode–endocardial interface, preventing boiling and ablation circuit impedance rise [2,5]. Several different electrode designs have been utilized [1–5]. No direct comparison between different electrode designs has been reported.

Herein, we present a comparison of three different irrigated electrode designs. An *in vitro* whole blood-superfused system designed to mimic the intracardiac environment was used. Electrode–endocardial interface and intramyocardial temperatures were measured and correlated with ablation circuit impedance and lesion morphology. Continuous echocardiographic monitoring of the interface was also performed. The influence of blood flow velocity on the function of each electrode design was examined.

Methods

Ablation Electrodes (Fig. 1)

Three different irrigated electrode designs were evaluated:

1. Internal: the electrode was 2.3 mm in diameter and 5 mm in length incorporating a thermocouple located 2.5 mm from the distal end of the electrode, which provided a measurement accuracy of ±2° C (Elecath, Inc., Rahway, NJ, USA). Irrigant fluid was circulated inside the electrode. The irrigation rate was controlled by a programmable motorized pump (Masterflex®, Cole Parmer Inc., Vernon Hills, Ill., USA), which delivered the irrigant at a constant volume cc/min.
2. Showerhead: the electrode was 2.3 mm in diameter and 5 mm in length incorporating a thermocouple located 2.5 mm from the distal end of the electrode, which provided a measurement accuracy of ±2°C (Biosense Webster, Inc., Diamond Bar, CA, USA). The irrigant fluid traveled through a center lumen and exited via each of 6 irrigation holes, each with a diameter of 0.4 mm located radially around the electrode 1 mm from the distal tip.

3. Sheath: the electrode was 2.3 mm in diameter and 5 mm in length incorporating a thermocouple located 2.5 mm from the distal end of the electrode, which provided a measurement accuracy of ±2°C (Biosense Webster, Inc., Diamond Bar, CA, USA). Irrigant fluid did not pass through the electrode, but instead was delivered via an external sheath (2.6 mm diameter) positioned with its distal edge 1 mm proximal to the proximal edge of the electrode.

In Vitro Ablation System (Fig. 2)

This protocol was approved by the Institutional Animal Care and Use Committee of the Allegheny University of the Health Sciences, and was in compliance with the Guide for Care and Use of Laboratory Animals published by the National Institutes of Health, publication number 78–83. Bovine smooth ventricular myocardium from freshly killed animals was mounted on an isolated ground plate at the base of a tank circulating bovine heparinized whole blood (10–12 liters) at 37°C. Thermocouples (T-type, 0.3 mm diameter; measurement accuracy ±2°C; Omega Engineering Inc., Stamford, CT, USA) were inserted at depths of 0 (electrode–endocardial interface, T_0), 1 (T_1), 3 (T_3), 5 (T_5) and 7 (T_7) mm. Each thermocouple was electrically insulated so as to eliminate artifact and prevent fluctuations of averaged temperatures >0.5°C root-mean-square in the radiation fields encountered herein. Each electrode was mounted on a force-transducer (AccuForce, Acme Scale Inc., San Leandro, CA, USA) and locked into position such that it was aligned perpendicular to the tissue, directly above the thermocouples. Approximately 20% of the electrode surface area was in contact with endocardium: this required slight variations in the applied force (approximately 0.1 Newton). Blood flow was directed to the electrode–endocardial interface using a pulsatile flow pump (Masterfiex, Cole Parmer Inc., Vernon Hills, Ill., USA) with a pulse rate of 60/min. When activated, the pump delivered blood so as to achieve a peak velocity of 0.26 m/s and a mean velocity of 0.20 m/s at the electrode–endocardial interface on the side of the electrode adjacent to the blood flow source. This is consistent with velocities commonly measured along the endocar-dial surface in man [6]. When the pump was inactivated, interfacial flow velocity was negligible. The interface was imaged using a multiplane transesophageal echocardiographic probe mounted into the tank (ATL, Bothell, WA, USA). Two-dimensional imaging was performed at a frequency of 5 MHz. A time calibration was employed to permit synchronization of echocardiography and temperature/impedance measurements. Prior to ablation, color and pulsed Doppler were utilized to describe the direction and magnitude of flow velocity along the electrode outer surface during irrigation without blood flow.

Radiofrequency energy (RF) was applied continuously in unipolar fashion between the ablation electrode and the ground plate utilizing a commercial generator (EP Technologies, Sunny-vale, CA, USA) operating at approximately 550 KHz. During each RF application, power, voltage, current, ablation circuit impedance and electrode/myocardial temperatures were measured continuously with sampling at 200 Hz using a commercial data acquisition system (Superscope II, GW Instruments Inc, Somerville, MA, USA). Data were digitized and stored.

Electrode and Lesion Morphology

After each RF application, the electrode was examined for coagulum [2,4,5,7]. The endocardial surface was inspected for disruption ("cratering") and coagulum [2,4,5,7,8]. The myocardium was then sectioned coronally and stained with 1% triphenyl tetrazolium chloride. This dye stains intracellular dehydrogenase, which distinguishes viable and necrotic tissue. Necrosis was observed when myocardial temperature exceeded 55°C for at least 10 seconds. The following lesion dimensions were measured using a caliper: maximum depth, maximum width, endocardial surface diameter, and depth at maximum width (Fig. 3). Lesion volume was calculated by assuming the lesion shape was an oblate ellipsoid and subtracting the volume extending above the surface of the tissue [5].

Experimental Protocol

Several different experimental groups were established (Table 1). Groups 1 and 2 were a non-irrigated "control" group, in which the showerhead electrode was utilized but was not irrigated. In Groups 3 (no blood flow) and 4 (blood flow), the internal electrode design was evaluated. In Groups 5 (no blood flow) and 6 (blood flow), the showerhead electrode design was evaluated. In Groups 7 (no blood flow) and 8 (blood flow), the sheath electrode design was evaluated. For all groups, RF power was fixed at 50 watts. RF duration was 60 s unless interrupted by a significant rise in ablation circuit impedance, defined as ≥10 ohms. Each electrode was irrigated with room temperature normal (0.9%) saline at a flow rate of 20 cc/min.

Analytical Methods

Data are expressed as mean ± standard deviation, unless otherwise specified. The biophysical parameters (power, impedance, current, voltage), temperatures, and lesion dimensions were compared between groups using one-way ANOVA (Student-Newman-Keuls) or unpaired 2-tailed *t*-test. For each statistical test, a P value of <0.05 was considered statistically significant.

Results

Echocardiographic Assessment of the Electrode Surface (Fig. 4)

Assessment of the non-irrigated electrode surface in the absence of blood flow revealed non-uniform flow without significant velocity. Assessment of the internal irrigation design surface during irrigation in the absence of blood flow showed no significant differences. Assessment of the shower-head irrigation design surface revealed much higher velocity flow. At the electrode holes, the peak flow velocity was 0.44 m/sec. The principal direction of the flow was *away* from the electrode surface, parallel to the endocardial surface, in a radial fashion. Away from the electrode holes, both proximally and at the electrode–endocardial interface, flow velocity was significantly lower (<0.1 m/s). Assessment of the sheath irrigation design surface revealed lower peak flow velocity (0.21 m/s). However, unlike the showerhead design, the principal direction of flow was parallel to and along the surface of the electrode, directly toward the endocardial surface (Fig. 1). The velocity profile was essentially uniform along the entire electrode surface.

Ablation Results (Tables 2, 3)

During RF applications using the non-irrigated electrode (Groups 1 and 2), T_0 rapidly approached 100°C, paralleled by T_E (Fig. 5). In Group 1, as both temperatures neared 100°C, two echocardiographic observations were made consistently: 1. the electrode diameter increased abruptly; 2. there was the sudden appearance of bubbles eminating from the interfacial region, associated with an audible “pop” and the initiation of a marked impedance rise, eliciting RF shutoff. In Group 2, the sudden appearance of bubbles occurred as in Group 1, but there was a slower increase in electrode diameter. This was associated with a delay in impedance rise, permitting higher total energy deposition, intramural temperatures, and lesion dimensions. In both groups, electrode and endocardial coagulum were observed consistently.

During RF application using the internal electrode design (Groups 3 and 4), T_0 rapidly approached 100°C, paralleled by T_E (Fig. 6). In Group 3, as T_0 neared 100°C, there was the sudden appearance of bubbles emanating from the interfacial region, associated with an audible “pop” and the initiation of a slow (relative to Group 1) increase i n e lectrode diameter. This was associated with a delay in impedance rise relative to Group 1, permitting higher total energy deposition, intramural temperatures, and lesion dimensions. In Group 4, the interfacial bubbling was observed early as in Group 5, but the increase in electrode diameter was further delayed. This was associated with a delay in impedance rise relative to Group 3, permitting higher total energy deposition, intramural temperatures, and lesion dimensions. In both groups, impedance rise occurred consistently, precipitating premature generator shutoff. Electrode and endocardial coagulum were observed consistently.

During RF application using the showerhead electrode design (Groups 5 and 6), T_0 rapidly approached 100°C; the rate of rise in T_E was similar, but the maximum value was significantly lower (Fig. 7). As T_0 neared 100°C, there was the sudden appearance of echocardiographic bubbles *without* a significant change in the electrode diameter. This was associated with an audible pop and the initiation of an insignificant (<10 ohms) impedance rise. Continued RF application was associated with progressive increase in intramural temperatures. In Group 5, a gradual, significant increase in the echocardiographic electrode diameter was observed in all trials. In concert with this, the impedance gradually rose. In 3 of 6 experiments, it eventually exceeded 10 ohms, eliciting premature generator shutoff. In Group 6, there was no significant change in the electrode diameter throughout the RF application period. Impedance was stable after the early minor rise and RF was delivered for the planned duration i n all experiments. Delay or elimination of a significant impedance rise in Groups 5 and 6 permitted greater total RF energy delivery than in Groups 3 and 4, associated with higher intramural temperatures and larger lesions. Endocardial coagulum was observed after most applications. Electrode coagulum was observed consistently in Group 5 but never in Group 6.

During RF application using the sheath electrode design (Groups 7 and 8), T_0 did not reach 100°C (Fig. 8). T_E was significantly lower than T_0. No echocardiographic bubbles were observed until T_1 approached 100°C, at which time there was an explosive release of bubbles associated with a n audible pop. These phenomena were coincident with the initiation of an insignificant impedance rise. Continued RF application was associated with

progressive increases in intramural temperatures. There were no changes in echocardiographic lesion diameter throughout the RF application period in either group. After the early insignificant rise, impedance was stable and RF was delivered for the entire planned duration in all trials. No electrode or endocardial coagulum was observed. There were no significant differences between the groups in total energy delivered, intramural temperatures, or lesion dimensions. Maximal lesion diameter was significantly greater in these groups than in all other groups.

Discussion

Biophysics of Irrigated Ablation

Confirming previous reports, in the present study RF application via each irrigated electrode design resulted in deeper and more voluminous lesions than a non-irrigated electrode. Compared with non-irrigated ablation, RF duration during irrigation was significantly longer; this was associated with greater total energy deposition and higher intramural temperatures. RF duration was increased due to delay or prevention of significant impedance rise but not necessarily prevention of interfacial boiling. Electrode coagulum was consistently associated with impedance rise; irrigation eliminated or delayed its formation.

Comparison of Electrode Designs

To our knowledge, this is the first direct comparison of ablation using different irrigated electrode designs. Significant differences in outcome were apparent. In the absence of blood flow, RF duration using the internal electrode design was significantly shorter than with showerhead or sheath designs, and resulting lesions were smaller. Echocardiographic assessment during RF demonstrated that the electrode surface of the internal irrigation design accumulated coagulum faster than the other designs. RF duration using the showerhead design was significantly shorter than the sheath design. The sheath design was the only electrode which: 1. did not accumulate coagulum during RF application; 2. prevented electrode–endocardial interfacial boiling; 3. prevented endocardial coagulum formation.

Echocardiographic assessment of the flow along the outer surface of each electrode may have provided insight as to why their biophysical profiles were different. During irrigation via the internal irrigation design, there was no significant flow along the electrode outer surface. During irrigation via the showerhead irrigation design, maximal electrode outer surface velocity was relatively high but localized to the electrode holes. Irrigant fluid was projected away from the electrode surface, and other areas of the electrode surface encountered much lower velocity. During irrigation via the sheath irrigation design, maximal irrigant velocity was less than 50% of the showerhead design. However, this velocity was uniform along the entire electrode surface. We hypothesize that the main mechanism by which irrigation prevented electrode coagulum formation (and thus impedance rise) was by creating flow along the electrode outer surface. This would act to protect blood components from sufficient exposure to elevated temperature to precipitate blood protein denaturation, the critical step in coagulum formation [9].

Our data demonstrate that augmentation of outer electrode surface flow was not the only mechanism by which irrigation mediates a larger lesion, given the longer RF duration, higher intramural temperatures and larger lesion dimensions relative to non-irrigated ablation. We speculate that the outer surface of the electrode during internal irrigation is cooled to some extent by the internal fluid flow, thereby delaying the formation of coagulum. We believe that this mechanism is of minor importance relative to flow augmentation on the outer electrode surface, based on several observations: 1. during irrigation prior to RF application, T_E in the internal irrigation design was significantly lower, yet T_0 was significantly higher, than the other designs; 2. during RF application, maximum T_E in the internal irrigation design was lower ($P < 0.05$ for comparison with showerhead design, $P > 0.05$ for comparison with sheath design) than the other designs; 3. despite equivalent electrode dimensions and irrigation volume in all electrode designs, the internal design yielded the smallest lesion dimensions; 4. RF application via the sheath irrigation design electrode, in which no irrigant flowed within the electrode, yielded the largest lesions. These observations also suggest that, during irrigation, internal electrode temperature may not accurately assess temperature on the outer electrode surface. The phenomenon of significant regional temperature heterogeneity in non-irrigated electrodes during RF application has been previously characterized [10–12].

Electrode and Lesion Morphology

There was a reduction in the incidence of electrode and endocardial coagulum associated with the sheath irrigation design electrode relative to the other designs. As discussed above, we believe that these disparities were due principally to the magnitude of flow encountered by the outer electrode and endocardial surfaces.

We also observed that the volume of lesions produced by the sheath irrigation design (Groups 7 and 8) was significantly greater than the other designs. Prolongation of RF duration relative to other designs, permitting greater total RF energy deposition, undoubtedly contributed to this finding. However, it could not have been the sole mechanism. For example, in Group 6 (shower-head electrode design, blood flow =0.26 m/sec), total RF energy deposition was identical to Groups 7 and 8. The main reason for the difference in lesion volume (an estimate) was a larger maximum lesion diameter (a direct measurement). We speculate that the effective sheath electrode width could have been larger than the actual electrode width, due to a “virtual” electrode effect provided by the saline traveling parallel to the electrode surface. A wider electrode would have been expected to create a wider lesion. The insignificant difference in endocardial surface lesion diameter between Group 6 and Groups 7/8 may appear to conflict with this hypothesis. However, we further speculate that the cooling effect of the irrigation might have prevented accumulation of ablative temperatures in more superficial myocardial regions. In support of this hypothesis, the endocardial–electrode interface with the sheath was cooler than the showerhead design both before and during RF application.

Influence of Blood Flow

In the absence of irrigation, blood flow was associated with lower electrode temperature, longer RF duration, greater total delivered energy and higher intramural temperatures.

During irrigation at 20 cc/min with the internal design, the introduction of blood flow was associated with longer RF duration, greater total delivered energy and higher intramural temperatures. During irrigation at 20 cc/min with the shower-head design, the introduction of blood flow was associated with lower electrode temperature, eradication of electrode coagulum, longer RF duration, greater total delivered energy and higher intramural temperatures. In contrast, during irrigation at 20 cc/min with the sheath design, the introduction of blood flow had no significant effect on biophysical parameters, intramural temperatures, or lesion dimensions. These data suggests that: 1. blood flow and irrigation have a similar biophysical effect (cooling of the electrode surface) which prevents coagulum formation and impedance rise, permitting longer RF duration; 2. Blood flow does not cause additional electrode cooling during irrigation with the sheath design.

Limitations

Our data have several limitations. First, we utilized an *in vitro* system in which the targeted myocardium was not perfused. Previous studies have demonstrated significant changes in myocardial properties soon after excision without perfusion [13]. Similarly, the *ex vivo* whole blood may have had properties, including rheologic and biophysical, which might be substantially different *in vivo.* Second, our observations may be specific to the RF power, duration, irrigant fluid content and irrigation rates utilized herein. Third, we evaluated only one manner of stable electrode–endocardial angulation and contact, utilizing smooth endocardium. Changes in these parameters may have significant effects on function, which may be variable based on electrode design. Finally, and most importantly, our data cannot define an “optimal” irrigation design. Indeed, each design was demonstrated to create larger lesions than a non-irrigated electrode. The constraints on RF power/duration and electrode–endocardial contact parameters introduced by the study protocol may have artificially facilitated one design and/or hindered another. For these reasons, we stress that our data may not be predictive of the relative safety and/or efficacy of ablation utilizing the various electrode designs in man. Regarding safety, it is worth noting that endocardial disruption was observed with each of the irrigation designs, a reminder that serious morbidity may result during clinical use of irrigated ablation with injudicious RF power titration.

Acknowledgments

The authors gratefully acknowledge the support and assistance of Dr. Jian-Fang Ren, Dr. Stephen M. Dillon, John J. Michele, and Dr. James P. Dilger.

Supported in part by a grant from Biosense-Webster, Inc., Diamond Bar, CA

References

1. Mittleman RS, Huang SKS, DeGuzman WT, Cuenoud H, Wagshal AB, Pires LA. Use of the saline infusion electrode catheter for improved energy delivery and increased lesion size in radiofrequency catheter ablation. Pacing Clin Electrophysiol. 1995; 18:1022–1027. [PubMed: 7659553]
2. Skrumeda LL, Mehra R. Comparison of standard and irrigated radiofrequency ablation in the canine ventricle. J Cardiovasc Electrophysiol. 1998; 9:1196–1205. [PubMed: 9835264]
3. Ruffy R, Imran MA, Santel DJ, Wharton JM. Radio-frequency delivery through a cooled catheter tip allows the creation of larger endomyocardial lesions in the ovine heart. J Cardiovasc Electrophysiol. 1995; 6:1089–1096. [PubMed: 8720209]

4. Peterson HH, Chen X, Pietersen A, Svendsen JH, Haunso S. Tissue temperatures and lesion size during irrigated tip catheter radiofrequency ablation. Pacing Clin Electrophysiol. 2000; 23:8–17. [PubMed: 10666748]
5. Nakagawa H, Yamanashi WS, Pitha JV, Arruda M, Wang X, Ohtomo K, Beckman KJ, McClelland JH, Lazzara R, Jackman WM. Comparison of in vivo tissue temperature profile and lesion geometry for radiofrequency ablation with a saline-irrigated electrode versus temperature control in a canine thigh muscle preparation. Circulation. 1995; 91:2264–2273. [PubMed: 7697856]
6. Ren J-F, Schwartzman D, Michele JJ, Li KS, Hoffman J, Brode SE, Lighty GW Jr, Dillon SM, Chaudhry FA. Lower frequency (5 MHz) intracardiac echocardiography in a large swine model: imaging views and research applications. Ultrasound Med Biol. 1997; 23(6):871–877. [PubMed: 9300991]
7. Petersen HH, Chen X, Pietersen A, Svendsen JH, Haunso S. Temperature-controlled irrigated tip radio-frequency catheter ablation. J Cardiovasc Electrophysiol. 1998; 9:409–414. [PubMed: 9581956]
8. Eick OJ, Gerritse B, Schumacher B. Popping phenomena in temperature-controlled radiofrequency ablation. Pacing Clin Electrophysiol. 2000; 23:253–258. [PubMed: 10709234]
9. Schwartzman D, Fischer WD, Spencer EP, Pariszhkaya M, Devine W. Linear radiofrequency atrial lesions deployed using an irrigated electrode: electrical and histologic evolution. Circulation. 1998:I-567.
10. Mirotznik MS, Schwartzman D. Inhomogenous heating patterns of commercial electrodes for radio-frequency catheter ablation. J Cardiovasc Electrophysiol. 1996; 7:1058–1062. [PubMed: 8930737]
11. Panescu D, Whayne JG, Fleischman SD, Mirotznik MS, Swanson DK, Webster JG. Three-dimensional finite element analysis of current density and temperature distributions during radiofrequency ablation. IEEE Trans Biomed Eng. 1995; 42:879–890. [PubMed: 7558062]
12. Wong WS, VanderBrink BA, Riley RE, et al. Effect of saline irrigation flow rate on temperature profile during cooled radiofrequency ablation. J Intervent Cardiac Electrophysiol. 2000; 4:321–326.
13. Schwartzman D, Chang I, Michele JJ, Mirotznik MS, Foster KR. Electrical impedance properties of normal and chronically infarcted left ventricular myocardium. J Intervent Cardiac Electrophysiol. 1999; 3(3):213–224.

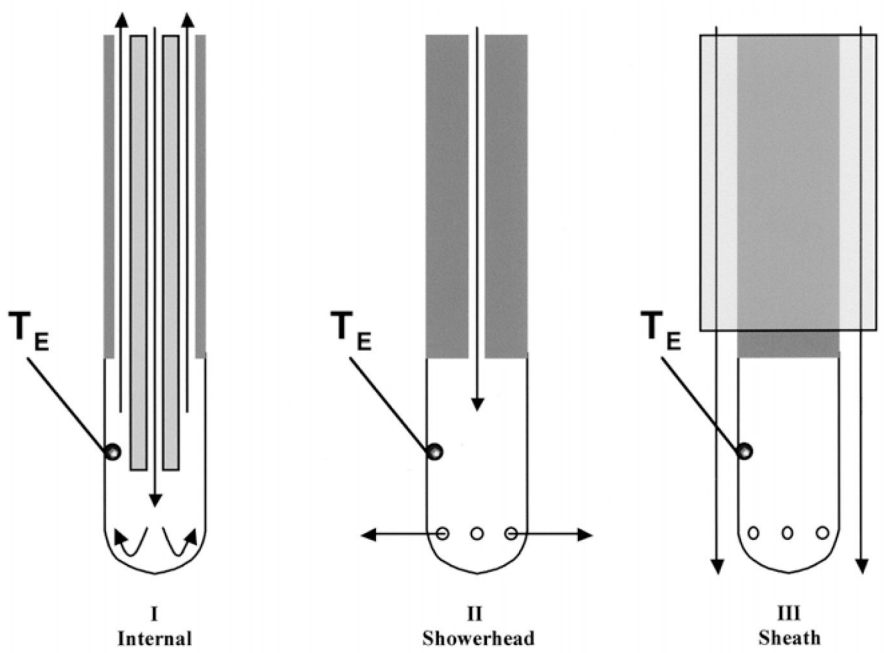

Fig. 1.

Cross-sectional schematics of the 3 irrigated electrode designs. Irrigant flow through the electrode is shown by the arrows. The location of the electrode thermocouple (T_E) is demonstrated. Note that the orientation of T_E was consistent, directly facing the blood flow source (see Fig. 2).

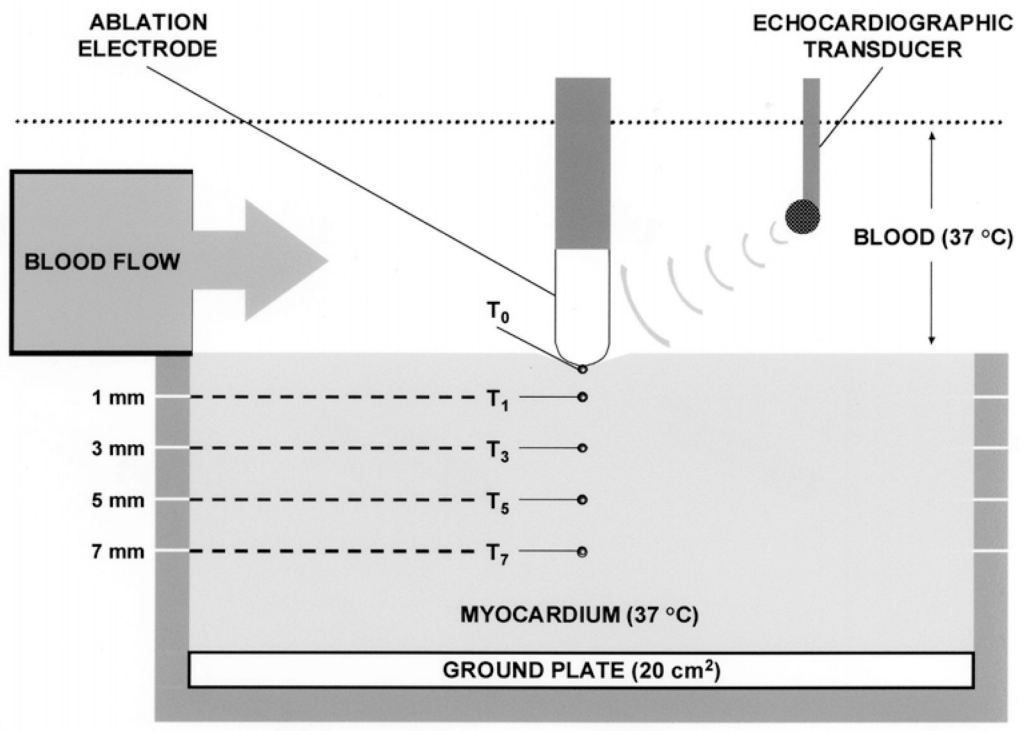

Fig. 2.
Schematic of in vitro ablation system.

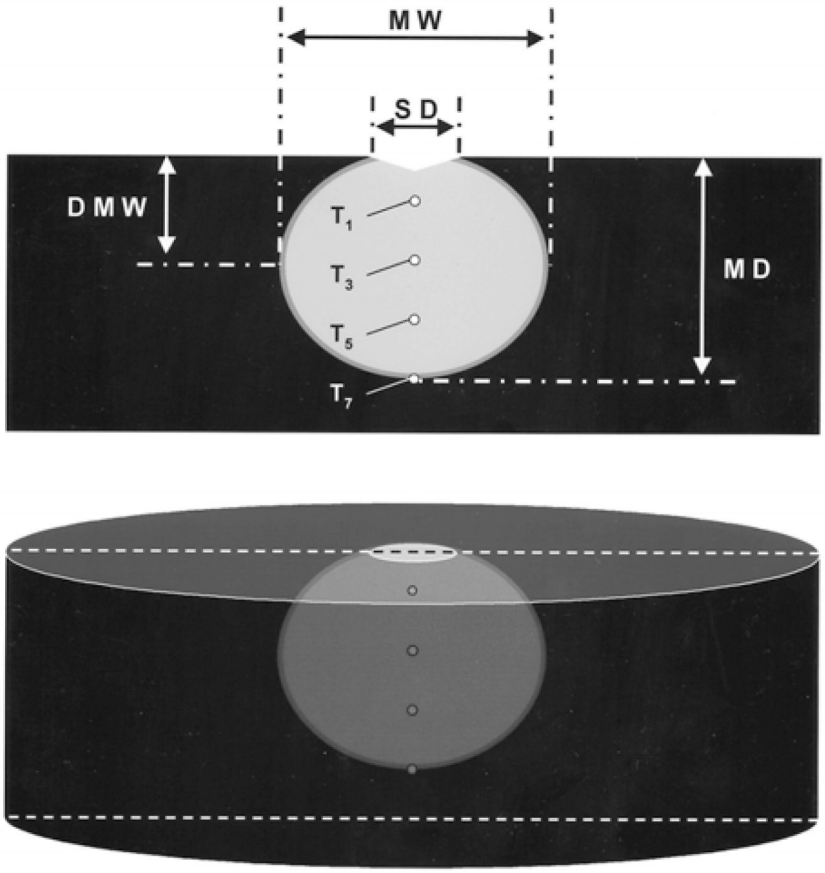

Fig. 3.

Schematic of ablation lesion, depicted as the light area with viable myocardium dark. MW =maximum width; SD = endocardial surface diameter; DMW =depth at which lesion width was maximal; MD =maximal depth.

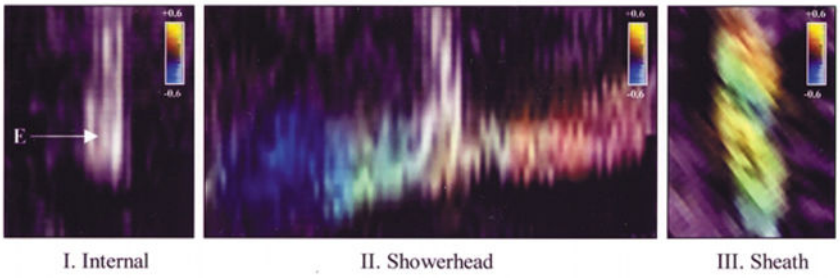

Fig. 4.

Color Doppler assessment of the direction of irrigant flow via the showerhead electrode design. Significant velocity denoting flow vector is seen coursing parallel to the endocardial surface (dotted line), directly away from the electrode surface.

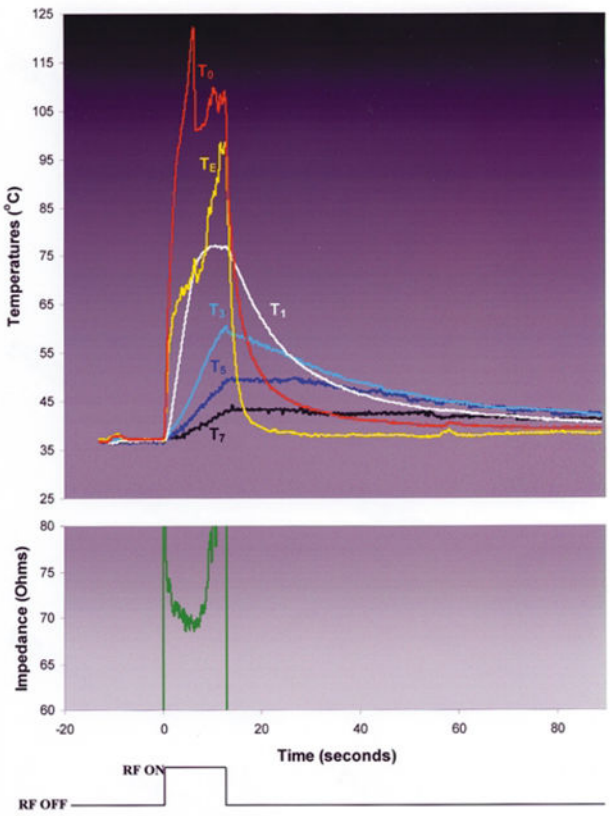

Fig. 5.

Typical trial in experimental group 2: non-irrigated electrode, blood flow 0.26 m/sec. Note that both T_0 and T_E rise rapidly to boiling, followed rapidly by a marked impedance rise and automatic generator shutoff.

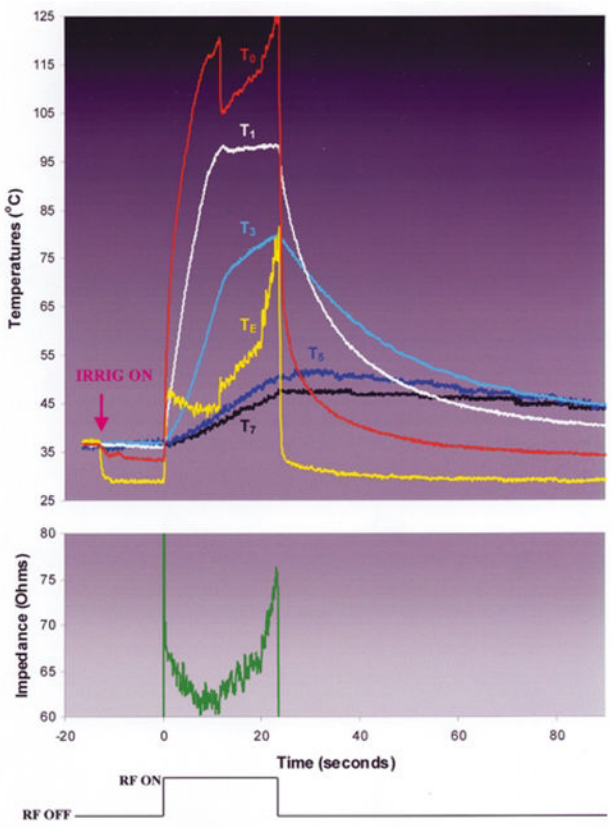

Fig. 6.

Typical trial in experimental group 4, internal irrigation design, blood flow =0.26 m/sec. Note that T_0 rises rapidly to boiling, at which point it abruptly deflects downward. This deflection was coincident with the sudden elaboration of echocardiographic bubbles at the electrode–endocardial interface and an audible “pop,” not associated with a significant impedance rise. Trials stopped at this instant (data not shown) showed displacement of the interface thermocouple to a site adjacent to the interface. After a few seconds, T_0 resumes its rise, but at a much slower rate. Note that despite the evidence of electrode–endocardial interfacial boiling, continued RF application is associated with progressive rise in intramural temperatures. Impedance rise subsequently reaches 10 ohms, precipitating premature generator shutoff.

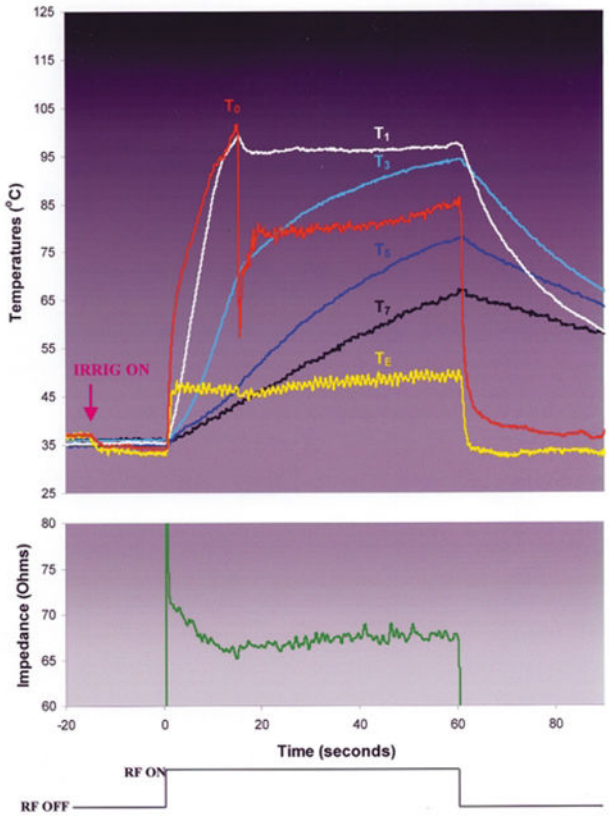

Fig. 7.

Typical trial in experimental group 6, showerhead irrigation design, blood flow =0.26 m/sec.

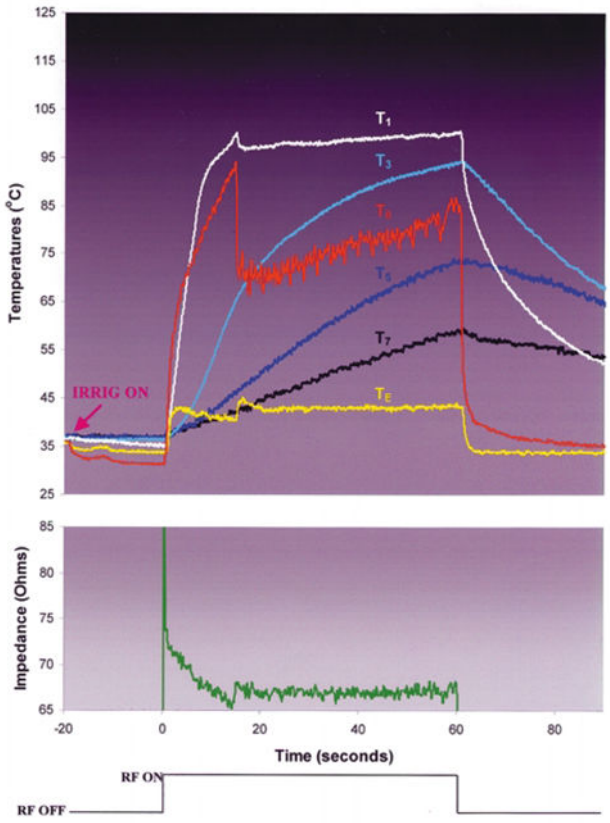

Fig. 8.

Typical trial in experimental group 8, sheath irrigation design, blood flow 0.26 m/sec.

Table 1

Experimental groups

Group	1	2	3	4	5	6	7	8
Number of trials (*n*)	5	6	7	5	6	6	7	5
Electrode design	NI	NI	INT	INT	SH	SH	Sheath	Sheath
T_0 target (°C)	–	–	–	–	–	–	–	–
Irrigant type	–	–	RTNS	RTNS	RTNS	RTNS	RTNS	RTNS
Irrigation rate (cc/min)	–	–	20	20	20	20	20	20
Blood flow velocity (m/s)	0	0.26	0	0.26	0	0.26	0	0.26
Delivered power (Watts)	50	50	50	50	50	50	50	50

NI =non-irrigated; INT =internal irrigation design; SH =showerhead irrigation design; Sheath =sheath irrigation design; RTNS =room temperature normal saline. Shaded columns refer to groups with blood flow velocity =0.26 m/sec.

J Interv Card Electrophysiol. Author manuscript; available in PMC 2018 January 23.

Table 2

Temperature data

Group	1	2	3	4	5	6	7	8
T_E	114 ±7 *	103±6	42±3 *a*	45 ±5 *b*	71 ±5	49 ±2 *b*	47 ±4 *ae*	44 ±2 *b*
T_0	114 ±3 *	121±5	115±5	120±9	98 ±7 *ac*	100 ±2 *bd*	80 ±14 *ace*	93 ±2 *ba*
T_1	65 ±12 *	77±11	89±11 *a*	96 ±2 *b*	98 ±6 *a*	99 ±6 *b*	102±4 *ac*	101 ±3 *b*
T_3	46 ±3 *	57±7	54±8	65 ±14	85 ±11 *ac*	92 ±3 *bd*	95 ±5 *ace*	96 ±4 *bd*
T_5	39 ±1 *	47±3	46±3	51 ±12	73 ±12 *ac*	81 ±5 *bd*	82 ±10 *ac*	81 ±6 *bd*
T_7	38 ±1	39±3	39±1 *	47 ±6 *b*	54 ±11 **ac*	67 ±6 *bd*	69 ±14 *ace*	66 ±6 *bd*

Maximum electrode (E), interface (0), and intramural (1, 3, 5, and 7 mm depth) temperatures (T), separated by experimental groups (columns). Shaded columns refer to groups with blood flow velocity =0.26 m/sec.

a P <0.05 vs Group 1;

b P < 0.05 vs Group 2;

c P <0.05 vs Group 3;

d P <0.05 vs Group 4;

e P <0.05 vs Group 5;

f P <0.05 vs Group 6

* P <0.05 vs matching group with blood flow (e.g., Groups 1 vs 2, 3 vs 4, 5 vs 6, and 7 vs 8).

J Interv Card Electrophysiol. Author manuscript; available in PMC 2018 January 23.

Table 3

Biophysical data

Group	1	2	3	4	5	6	7	8
Baseline impedance (Ω)	83±4	80 ±3	72±2 *a	68 ±2 b	84 ±7 c	81 ±1 d	73 ±3 ae	74 ±2 bdf
Mean voltage (V)	65±8	58 ±1	58±3	56 ±1 b	60 ±5	58 ±1 d	60 ±2	57 ±1
Mean current (A)	1±0.03	0.9±0.003	1±0.01	0.9±0.007	0.9±0.02	0.9 ±0.003	1±0.007	0.9±0.003
RF Duration (s)	7±5 *	15 ±2	16±5 *a	32 ±16 b	49 ±12 *ac	60 ±0 bd	60 ±0 ace	60 ±0 bd
Total delivered energy (J)	345±105 *	746±123	808±256 *a	1583 ±806 b	2473 ±585 ac	3000 ±0 bd	3000±0 ace	3000 ±0 bd
Audible pop (*n*)	4	6	7	5	6	6	7	5
Significant (>10 Ω) impedance rise (*n*)	5	6	7	5	6	0	0	0
Echacardiographic explosion (*n*)	5	6	7	5	6	6	7	5
Electrode coagulum (*n*)	5	6	7	5	6	0	0	0
Endocardial coagulum (*n*)	3	6	7	5	4	6	0	0
Endocardial disruption (*n*)	0	0	0	1	1	0	0	1
Lesion depth (mm)	2.6±0.2 *	4.2±.3	4.0±0 *a	5.0±1	7.0±1.3 ac	7.6 ±0.8 bd	8.0±1 ace	8.0±0 bd
Lesion width (mm)	6.8±0.8 *	9.0±0	7.0±1 *	9.0±1	10.0 ±0 ac	10.0 ±0 bd	13.0±2 ace	13.0 ±1 bdf
Depth at max width (mm)	0.0±0 *	0.8±0.3	0.1±0.2 *	1.5±0.8 b	2.4±1.5 ac	2.8 ±0.4 bd	2.8±0.4 ace	3.2±0.3 bd
Surface diameter (mm)	5.8±0.8	6.1±0.9	6.6±1.3	6.8±0.8	5.6±1.7	6.8 ±1.3	7.4±1.7	7.0±0.0
Lesion volume (mm^3)	54±14 *	141±11	81±18 *	148±34	251±10 ac	263 ±36 bd	463±121 ace	462±41 bdf

Shaded columns refer to groups with blood flow velocity 0.26 m/sec.

[a] P <0.05 vs Group 1;

[b] P < 0.05 vs Group 2;

[c] P <0.05 vs Group 3;

[d] P < 0.05 vs Group 4;

[e] P <0.05 vs Group 5;

[f] P < 0.05 vs Group 6;

* P <0.05 vs matching group with blood flow (e.g., Groups 1 vs 2, 3 vs 4, 5 vs 6 and 7 vs 8).